Supporting Information

Short Peptide-based Cross-β Amyloids Exploit Dual Residues for Phosphoesterase like Activity

Chiranjit Mahato[a], Sneha Menon[b], Abhishek Singh[a], Syed Pavel Afrose[a], Jagannath Mondal[b], and Dibyendu Das[a]*

[a] Department of Chemical Sciences & Centre for Advanced Functional Materials, Indian Institute of Science Education and Research (IISER) Kolkata, Mohanpur, West Bengal, 741246, India
E-mail: dasd@iiserkol.ac.in

[b] Tata Institute of Fundamental Research Hyderabad, Telangana 500046, India.

Table of Contents

1. Materials

DIPEA (N,N-diisopropylethylamine), activator DIC (N,N' Diisopropylcarbodiimide), Trifluoroacetic acid (TFA), sodium borohydride, gold chloride trihydrate, and trisodium citrate dehydrate and all of the fluorenylmethyloxycarbonyl (Fmoc) protected amino acids, Amberlite IR-120 (Hydrogen form) were purchased from Sigma Aldrich. Oxyma pure was acquired from Nova Biochem. p-Nitrophenylphosphate Disodium Salt Hexahydrate (PNPP) was purchased from SRL. Bis(p-nitrophenyl) phosphate was purchased from TCI chemicals. All solvents and Fmoc-Rink amide MBHA Resin were purchased from Merck. Milli-Q water was used throughout the experiments.

2. Methods

Synthetic procedure of peptides

RLVFFA**H** and all control peptides were made using automated Aapptec peptide synthesizer. Fmoc-Rink Amide MBHA Resin having loading capacity of 0.52 mmol/g, was swollen for 15 minutes in DMF before starting Fmoc-deprotection reaction. Afterward, deprotection was done by using 20% piperidine in DMF. The coupling reaction of every Fmoc–amino acid was carried out by using an activator (DIC) and oxyma pure solution in DMF. Lastly, the resin was washed with DMF and DCM for all peptides and allowed to dry in air. Trifluoroacetic acid (TFA)/Triethylsilane (5:0.1 v/v) were used to cleave the peptides from resin by keeping at room temperature for 2 hours. The final peptide-TFA solutions was filtered and followed by TFA removal by using a high vacuum and precipitated by dropwise addition to the cold ether. The precipitated was centrifuged at 8000 rpm at 4 °C for 15 min in Eppendorf centrifuge 5804 R which resulted in white pellet formation. Pellet was washed 3 times more using cold diethyl ether. The obtained crude peptides were purified in preparative Waters HPLC system by using Atlantis T3 C18 preparative reverse phase column with a linear gradient of 0.1% TFA containing water and 0.1% TFA containing acetonitrile. Molecular weight was confirmed by Bruker Mass Spec Q-tof systems.

Ac-**R**LVFFA**H**-NH_2 (**RH**) ($C_{49}H_{73}N_{11}O_8$) (m/z) calculated for [M+H$^+$]: 944.57; found: 944.58

Im-**R**LVFFA**L**-NH_2 (Im-**RL**) ($C_{49}H_{73}N_{13}O_8$) (m/z) calculated for [M+H$^+$]: 972.57; found: 972.58

Ac-**H**LVFFA**L**-NH_2 (**HL**) ($C_{46}H_{66}N_{10}O_8$) (m/z) calculated for [M+H$^+$]: 887.51; found: 887.51

Ac-**R**LVFFA**L**-NH_2 (**RL**) ($C_{46}H_{66}N_{10}O_8$) (m/z) calculated for [M+H$^+$]: 906.5560; found: 906.5555

Synthesis of Negatively Charged gold nanoparticle

Negatively-charged gold nanoparticles (Neg-AuNP) were synthesized according to previously reported literature.[1] Briefly, 1250 µL of 1 mM stock solution of sodium citrate was added to the 2.5 mL of Mili-Q water and 1250 µL of $HAuCl_4$ (1 mM) was added with constant stirring. After that, 150 µL of 100 mM ice cold $NaBH_4$ added dropwise to the solution with continuous staring. Instantaneous appearance of orange-red colour was observed with a localized surface plasmon resonance (SPR) transmission at 512 nm in UV spectrum suggesting the formation of gold nanoparticles. The average particle size was found to be 4±1 nm from transmission

electron microscopy (TEM). The final concentration of $HAuCl_4$ and Sodium citrate was 0.24 mM each, and $NaBH_4$ concentration was 2.91 mM.

Synthesis of 2-hydroxypropyl (4-nitrophenyl) phosphate (HPNPP)

HPNPP was synthesized using previous literature.[2] Briefly, p-Nitrophenylphosphate Disodium Salt Hexahydrate (PNPP) (1.32 g., 5 mmol) was dissolved in water (10 ml.), yielding a yellow solution which was passed through the pre-recharged column of IR-120 (H+) resin. The eluent was collected in several portions; small samples were spotted on TLC plate plates and viewed under UV lamp to identify the presence of 4-nitrophenyl phosphate. The aqueous portion of 4-nitrophenyl phosphate (colourless) was collected in a two-neck round bottom flask and the pH was adjusted to 8 by using aqueous ammonia (very light yellow at pH=8). After that, 1,2-epoxypropane (20 ml) was added dropwise to aqueous solution of 4-nitrophenyl phosphate at 35°C under refluxing conditions and kept it for 40 hrs. Unreacted epoxide was removed in rotary evaporator, and the bright yellow solution passed aging through the pre-recharged IR-120 (H+) column. The solution was neutralised by using carbonated free freshly prepared $Ba(OH)_2$ solution (pH should not be greater than 7 and try to avoid bright yellow colour generation). The solution was lyophilised and reduce the volume to 5 ml. Subsequently, 20 ml of ethanol was added to precipitate the unreacted 4-nitrophenyl phosphate. White precipitate of unchanged 4-nitrophenyl phosphate was filtered off. The solution was evaporated in a rotary evaporator to remove ethanol and put on lyophilization to yield an oily residue. 10 mL of 20% ethanol in acetone was added dropwise with constant stirring to the oily residue, forming a pure white precipitate. The precipitate was collected by filtration (220 mg).

A small portion of barium salt (49 mg, 0.18 mmol) was dissolved in 5 ml water in a centrifuge tube and to it, 500 µL of 0.14M Na_2SO_4 was added dropwise to convert the barium salt into sodium salt. A cloudy white solution appeared. After centrifugation for 30 min, the clear solution was separated from solid $BaSO_4$ and taken in a round bottom flask. After that, the clear solution was lyophilized to get white powder of sodium salt of HPNPP.

^{1}H NMR (400 MHz, D_2O) δ (ppm): 1.17 (d, 3H), 3.80-3.87 (m, 1H), 3.93-4.06 (m, 2H), 7.37 (d, 2H), 8.28 (d, 2H)

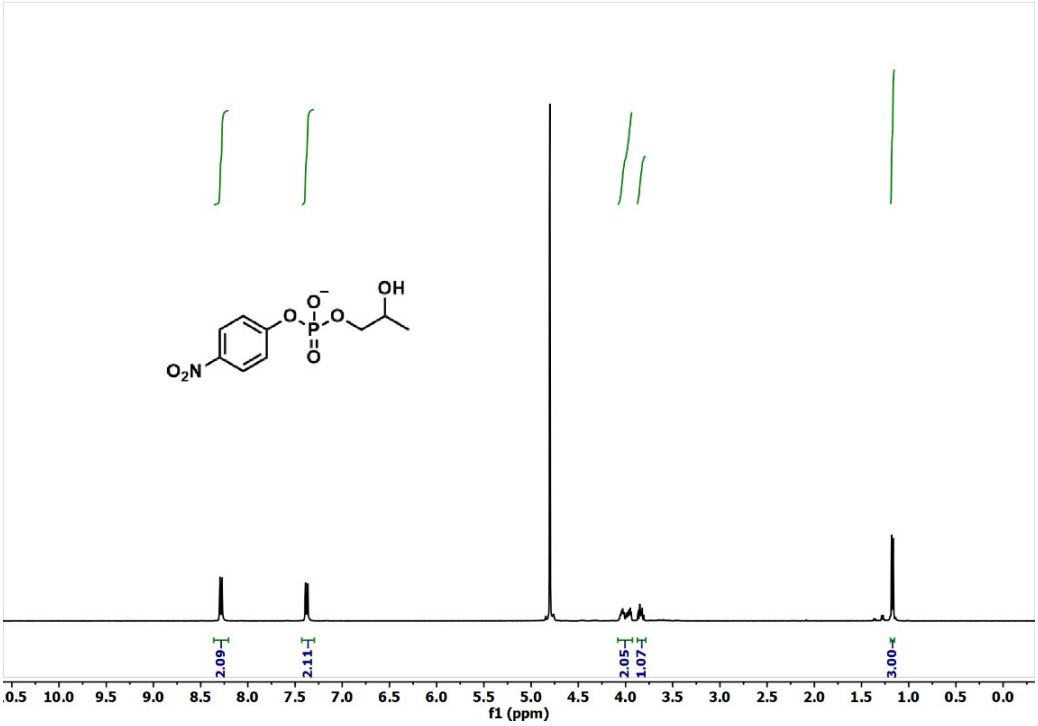

^{1}H NMR of HPNPP.

3. Experimental technique

Peptide assembly

The dried peptide powder of the peptides expect was dissolved in 40% ACN-H_2O (containing 0.1% TFA). Subsequently, 1 N NaOH was added carefully to maintain the pH 8 (except HL where the pH was 2). The homogeneous dissolved mixture was kept at 4°C a month to form proper assembly before use.

Redispersion technique

1 mL of 2.5 mM of assembled peptide solution was taken in a microcentrifuge tube (1.5 mL) and centrifuged at 12000 rpm for 30 min at room temperature in neuation i-Fuge D12 centrifuge. The pellet was formed after the centrifugation. After that, the supernatant was removed and the same amount of mili-Q water was added to disperse the pellet in water.

Transmission Electron Microscopy (TEM)

After one month of incubation in 40% acetonitrile-water, peptide assembly was diluted to 300 µM in mili-Q water and drop casted on a TEM grid and kept for 1 min. After adsorption, the extra solvent was wicked off cautiously using the filter paper. Afterward, 2 µL of 1 % (w/v) uranyl acetate was added on the TEM grid followed by incubation for 2 min and the extra solution was wicked off. After that, samples were retained in a desiccator for 4-5 hrs to dry the samples completely. TEM micrographs were taken with a JEOL JEM 2100 with a Tungsten filament. Accelerating voltage was kept at 200 kV during the experiment.

Gold Nanoparticle binding studies

At pH ~7 in water: 200 µL 0.24 mM of positively charged AuNP was incubated with 2.5 µL of 2.5 mM RH assembly and was kept for 5 h in incubation. After precipitation was observed, the

mixture was centrifuged to form pellet. Supernatant was discarded and dispersed with 39 µL of water. 10 µL of this mixture was casted on the TEM grid. Final concentration of peptide was 159.5 µM and AuNP = 1.23 mM.

At pH 5.5 (citrate buffer): 200 µL of 0.24 mM of positively charged AuNP was added to 200 µL of citrate buffer to maintain the pH 5.5. After that, 5 µL of 2.5 mM RH assembly was added to the mixture and incubated for 5 h, leading to formation of brown precipitate. After that, the system was centrifuged and dispersed with 78.33 µL of water. 10 µL of the dispersed solution was then casted on the TEM grid. The final concentration of peptide=159.5 µM and AuNP concentration=612.79 µM.

Atomic Force Microscope (AFM)

Samples were drop-casted on silicon wafers and were air-dried. The air-dried samples were scanned under ambient conditions using Bruker Multimode 8 scanning probe microscope, which was operated in tapping mode with a Nanoscope V controller and a J-scanner.

Circular Dichroism

CD spectra were recorded at 25 °C using a JASCO J-810 circular dichroism spectrometer fitted with a Peltier temperature controller. 400 µL of 2.5 mM peptide samples were added in a quartz cuvette of 1 mm path length and each spectrum was recorded by scanning wavelengths from 600 nm to 190 nm at a scanning rate of 100 nm/min.

Fourier-Transform Infrared Spectroscopy

Sample aliquots were dried as a thin film and IR spectra were recorded at room temperature using Bruker (model no: Alpha) in ATR mode (Platinum ATR) by averaging 256 scans with 4 cm^{-1} resolution. For each sample, the background spectrum was deducted.

Powder X-ray diffraction (PXRD)

1 mL of 2.5 mM RH assembly was centrifuged which led to formation of a white pellet. The supernatant was discarded and the pellet was freeze dried to get white powder. This lyophilized dry residue was used for the PXRD experiment. The XRD measurements were performed with a Rigaku (mini flex II, Japan) powder X-ray diffractometer having Cu Kα = 1.54059 Å.

Confocal Microscopy

Firstly, a mixture of 2 µL coumarin 343 dye (5 mM stock) and 20 µL of the peptide (2.5 mM stock) was incubated for 30 min and the solution was cast on a glass slide and was enclosed with a cover glass and excited by 458 nm laser line at an emission bandwidth of 493-560 nm. The images were recorded in Olympus Laser Scanning Confocal System Model FV3000 (part of the Atomic Force Microscope with Rheological Measurement and Confocal Imaging Unit facility, supported by Swarnajayanti (SB/SJF/2020-21/08)).

Activity measurement

The activity of the peptide assemblies were monitored in the Agilent Cary 8454 UV-Visible spectrophotometer/Cary 3500 (G9864A) UV-Vis spectrophotometer with the different substrates using pH 7 buffer (HEPES, 10 mM) at 40°C. Briefly, 4.4 µL of the peptide

assemblies (2.5 mM stock) were taken in 10 mM HEPES buffer in a microvolume quartz cell of 10 mm path length. This was followed by adding several concentrations of substrates (10 μM to 2 mM for HPNPP and PNPP, 10 μM to 500 μM for BNPP, 20 mM stock in water) at 40°C. Kinetic parameters (k_{cat} and K_M) were obtained by fitting the data to the Michaelis–Menten equation {$v_0 = k_{cat}[E]_0[S]_0/(K_M + [S_0])$}. For the control system, 4.4 μL of peptides (2.5 mM stock) was added with 2.75 μL of the substrate (20 mM stock) in 102.85 μL buffer (10 mM, pH 7) at 40°C. The absorbance change was monitored by the formation of p-nitrophenol, at λ_{max} = 405 nm (ε at 405 nm is 9100 M^{-1} cm^{-1}).[3]

HFIP Study

500 μL of RH assembly was centrifuged to make pellet and supernatant was discarded. After that, 400 μL of HFIP was added to the pellet and was kept for two hours to break the assembly. HFIP was removed by N_2 blowing and dried in a vacuum. 500 μL water was added to the dried film of the disassembled peptide to maintain the final concentration of 2.5 mM and was immediately used for activity monitoring.

Computational methods

Molecular Dynamics Simulations and Molecular Docking

A model of the Ac-**R**LVFFA**H**-$CONH_2$ assembly consisting of 4 laminates each with 6 hydrogen-bonded peptides in anti-parallel β-sheet arrangement was used as the starting structure to perform all-atom simulations. The peptides were modelled using the CHARMM36 force field[4] and solvated in a dodecahedron box containing 12259 water molecules of the TIP3P water model.[5] The system was neutralised by adding 24 chloride counterions. All-atom molecular dynamics (MD) simulations of the system was performed using the GROMACS 2018 simulation package.[6] The leap-frog MD integrator with a timestep of 2 fs was used to perform simulations in the isothermal-isobaric (NPT) ensemble. The particle mesh Ewald (PME) method [7] was used to calculate long-range electrostatic interactions with a cutoff of 12 Å and the covalent hydrogen bonds were contrained using the LINCS algorithm.[8] The simulation was performed at 300 K by employing the v-rescale thermostat[9] and pressure coupling at 1 bar was achieved using the Parrinello-Rahman barostat.[10] The system was first minimized using the steepest descent algorithm followed by equilibration, first in the isothermal-isochoric (NVT) ensemble and then in the NPT ensemble by applying position restraints on the heavy atoms of the protein. The production run was performed in the NPT ensemble for a timescale of 200 ns. Three independent MD simulations were performed for the fibrillar system.

Molecular Docking

A structure of the assembly obtained from the equilibrated trajectory was used as the receptor for performing docking calculations with the three substrate molecules namely, HPNPP, PNPP and BNPP. Molecular docking of the substrate molecules to the assembly was performed using the AutoDock Vina program[11] widely used for protein-ligand docking to predict accurate binding-mode predictions. The three-dimensional structures of the substrate molecules were created using chem3D. The topological PDBQT files of the substrate and the receptor i.e. assembly were generated using AutoDock Tools. The search space is defined as a grid box centered at 58.426, 72.270, 0.594 coordinates and dimensions in the x, y and z directions that covers the whole assembly was used. Ten iterations of docking were performed and the

docking conformation corresponding to the lowest docked energy was used was evaluated. The location of predominant docked pose on the surface of assembly was determined for redocking to validate the predicted docking mode. For redocking, the search space is restricted to the substrate binding site in the predominant docking pose. The ligand-protein interactions in the redocked pose is assessed by using the Protein-Ligand Interaction Profiler.[12]

Electronic Structure Quantum Calculations

Quantum chemical calculations were performed using the Gaussian16 program[13] to understand the underlying energetics of the reactions. Geometry optimisations and single point energy calculations were performed using M062X/6-31G(d) and M062x/6-311++G(d,p) levels of theory respectively. Geometry optimisations and TS optimisations were all performed using implicit solvation model enabled using the polarizable continuum solvation model (PCM)). Frequency Calculations were performed on all the structure to make sure the minima of reactants (absence of negative frequency) and transitions states (single negative frequency). Single point energy calculations provide the electronic energy of the system (E_0), while the zero-point vibrational energy (ZPVE) was added to the systems obtained from the frequency calculations to accurately represent the system at 0K. Finally thermal energy corrections were performed to get the enthalpies which were used further for the Gibbs free energies.

Enthalpies were calculated using the following equation:

$$\Delta H^{\ddagger} = \left(E_0 + ZPVE + TC\right)_{TS} - \left(E_0 + ZPVE + TC\right)_{reactants}$$

A reasonable starting structure for the catalysed process was obtained using the following process: The structure of the catalyst substrate complex obtained from the molecular dynamics simulations were used. A cut off radius of 10 Å was used to extract all catalytic moieties in all directions of the substrate. Finally the closest catalytic residues (imidazole and arginine) were chosen (6 Å) from the modified file and truncated using -NH_2/-CH_3 groups at the end of the chosen radius. The structures thus obtained were optimised to search for the minimum energy conformation using M062X/6-31G(d). The resultant structure was used as reactant and single point energy calculations were performed.

For transition state calculations, simple analogues without the catalysts were optimised by forming guess transitions states and optimised either using TS Berny Optimization Algorithm or the Synchronous Transit-Guided Quasi-Newton (STQN) Method whichever yielded the transition state. For catalysed process complex potential energy surface was dealt with investigating the whole potential energy surface by moving respective atoms by 0.05 Å involved in formation and breaking of the bond. Geometries on the maxima thus obtained on potential energy surface were used to find the TS by using Berny optimisation.

Table S1: The kinetic parameters of **RH** assembly for the hydrolysis of HPNPP.[14]

Catalyst	V_{max}(×10^{-9} M.s^{-1})	k_{cat}(×10^{-5} s^{-1})	K_M(×10^{-3} M)	k_{cat}/K_M (M^{-1}.s^{-1})	k_{rel}
RH	4.45±0.54	4.45±0.54	0.70±0.20	0.063	2.22×10^2

Where $k_{rel}=k_{cat}/k_{uncat}$.

Table S2: The kinetic parameters of **RH** assembly for the hydrolysis of PNPP.[15]

Catalyst	V_{max}(×10^{-8} M.s^{-1})	k_{cat}(×10^{-4} s^{-1})	K_M(×10^{-3} M)	k_{cat}/K_M (M^{-1}.s^{-1})	k_{rel}
RH	1.09±0.03	1.09±0.03	0.069±0.010	1.58	1.46×10^2

Where $k_{rel}=k_{cat}/k_{uncat}$.

Table S3: The kinetic parameters of **RH** assembly for the hydrolysis of BNPP.[16]

Catalyst	V_{max}(×10^{-9} M.s^{-1})	k_{cat}(×10^{-5} s^{-1})	K_M(×10^{-3} M)	k_{cat}/K_M (M^{-1}.s^{-1})	k_{rel}
RH	2.88±0.32	2.88±0.32	0.05±0.02	0.57	2.4×10^4

Where $k_{rel}=k_2$ *(cat)*$/k_2$ *(uncat)*.

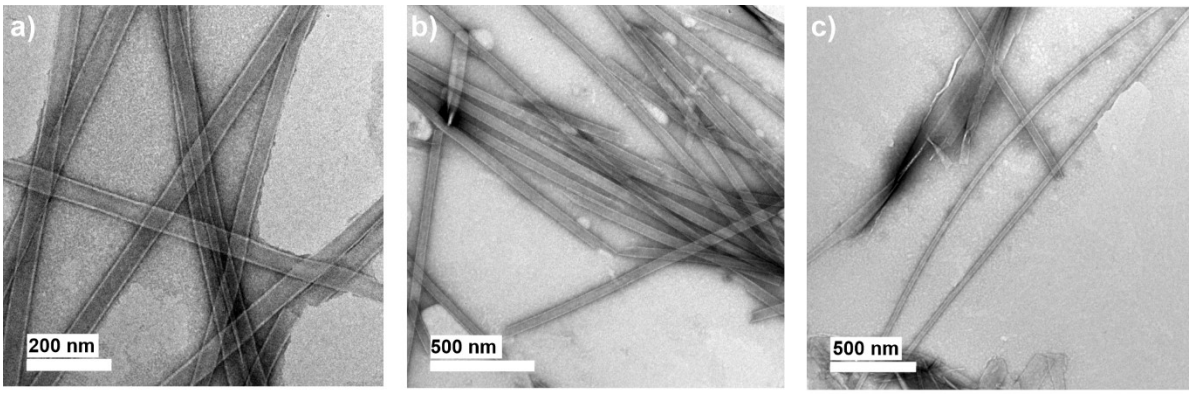

Figure S1. TEM micrographs of (a) **RL**, b) **HL** and (c) Im-**RL**.

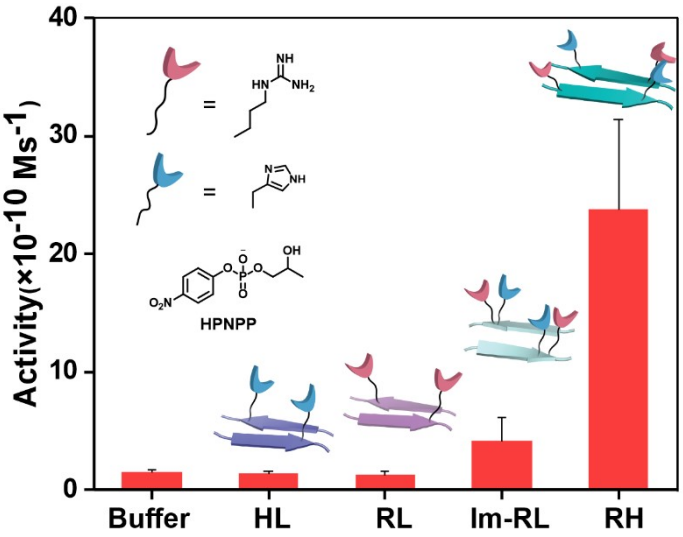

Figure S2. Bar diagram of initial rate of HPNPP hydrolysis by only buffer (40°C, pH 7, 10 mM HEPES), **HL**, **RL**, Im-**RL** and **RH**, [Peptide]=100 μM, [HPNPP]=500 μM.

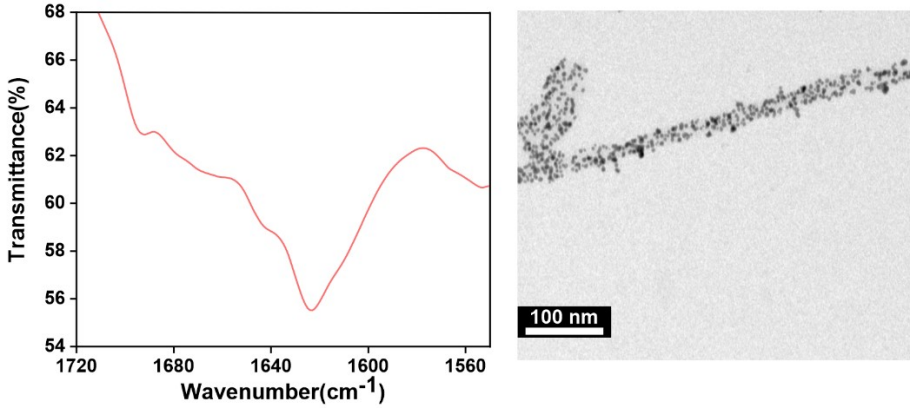

Figure S3. FTIR spectra of Im-**RL** (left) and TEM micrograph of negatively charged AuNP bound Im-**RL** (right).

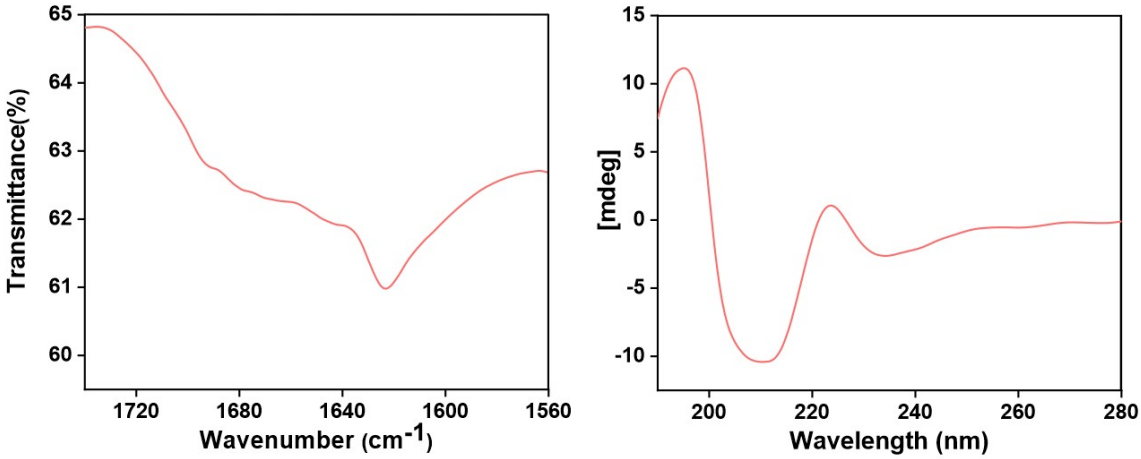

Figure S4. FTIR (left) & CD (right) spectrum of **RH** assemblies.

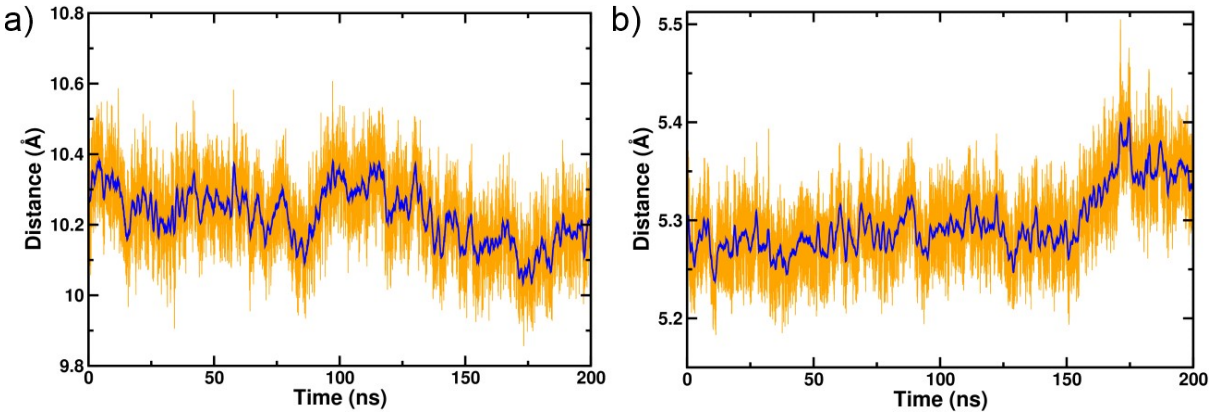

Figure S5. (a) Laminate distance and (b) interstrand distance of the **RH** assembly averaged over three simulation trajectories.

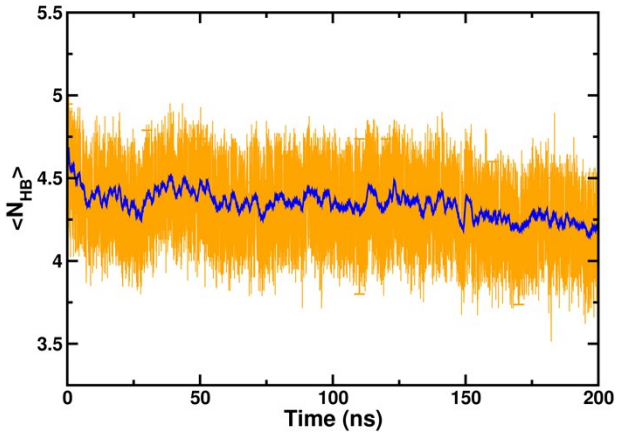

Figure S6. Mean number of interstrand hydrogen bonds (<N_{HB}>) in the **RH** assembly.

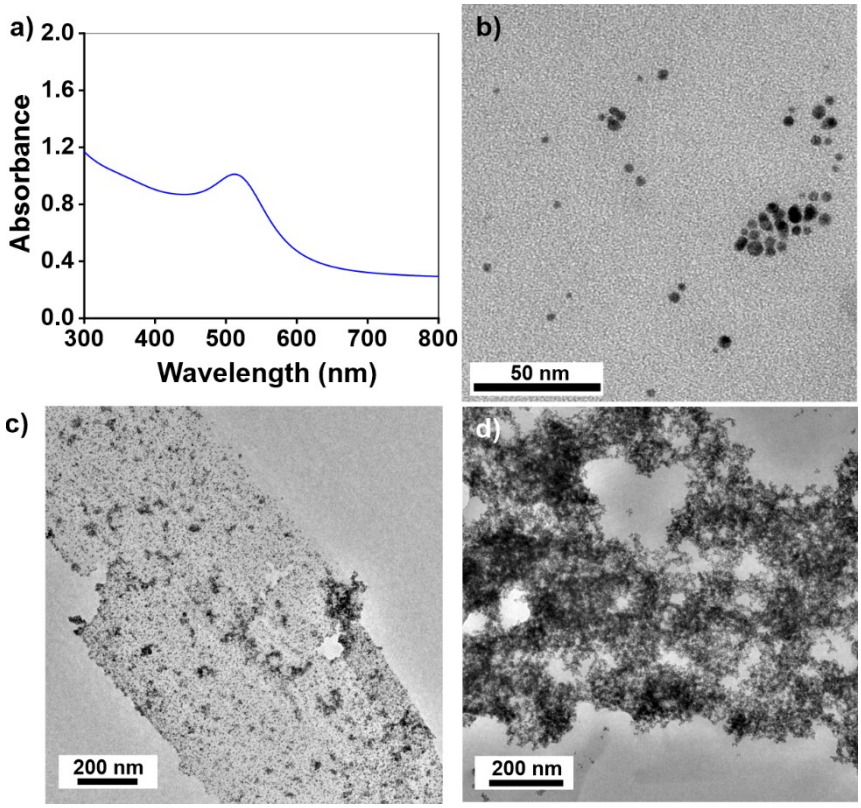

Figure S7. a) UV-Visible spectrum representing surface plasmon resonance (SPR) transition of negatively-charged citrate capped gold nanoparticle. b) TEM images of AuNPs. TEM image of negatively charged AuNP bound **RH** at c) pH 7 and d) pH 5.5.

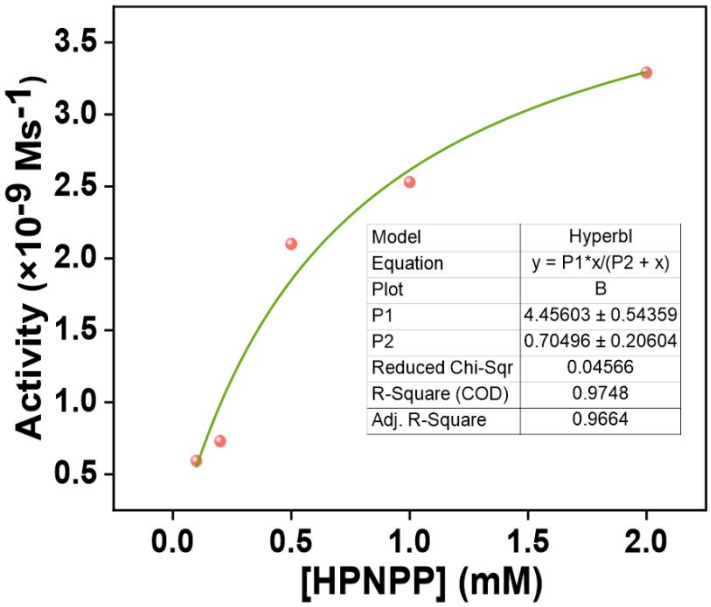

Figure S8. Representative Michaelis-Menten plot of **RH** for HPNPP substrate.

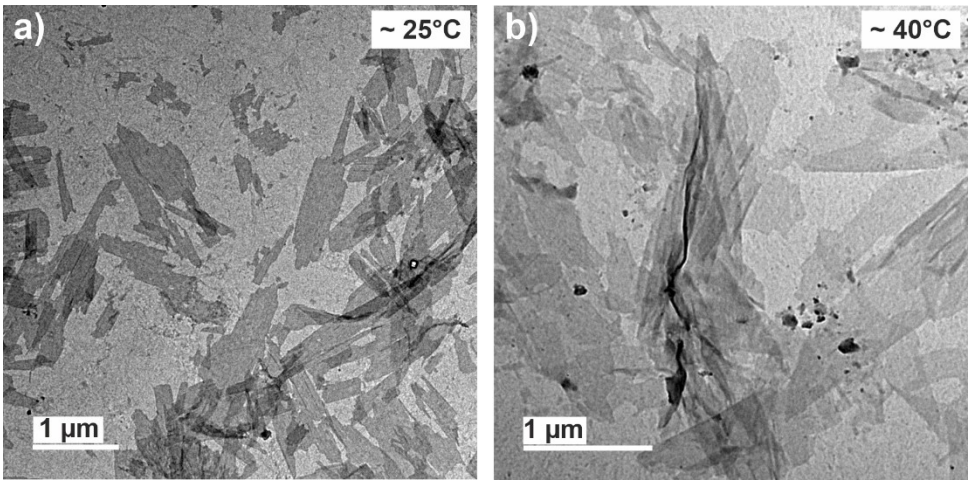

Figure S9. a) TEM images of **RH** kept at room temperature and b) after keeping at 40°C for 24 hours.

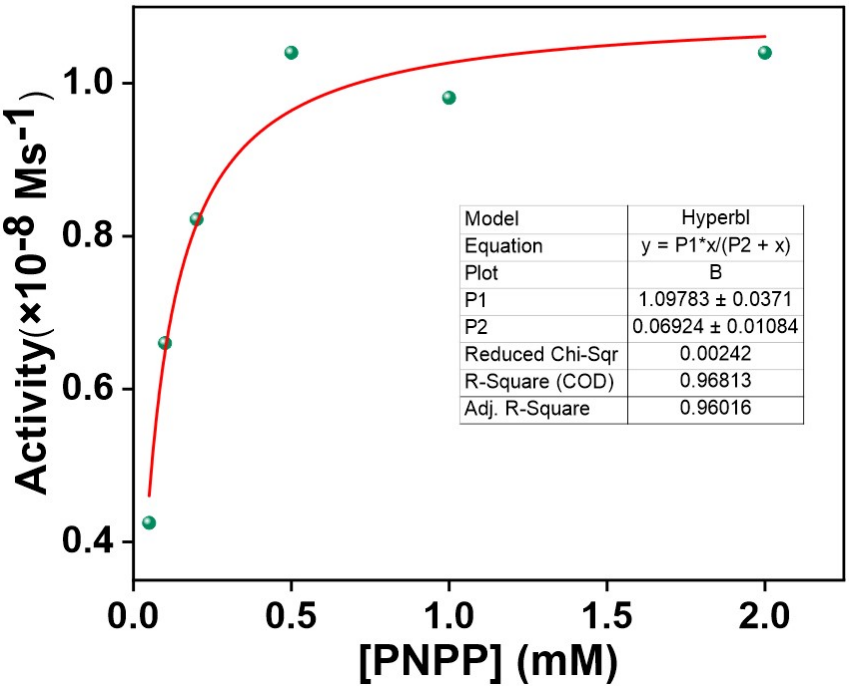

Figure S10. Representative Michaelis-Menten plot of **RH** for PNPP substrate.

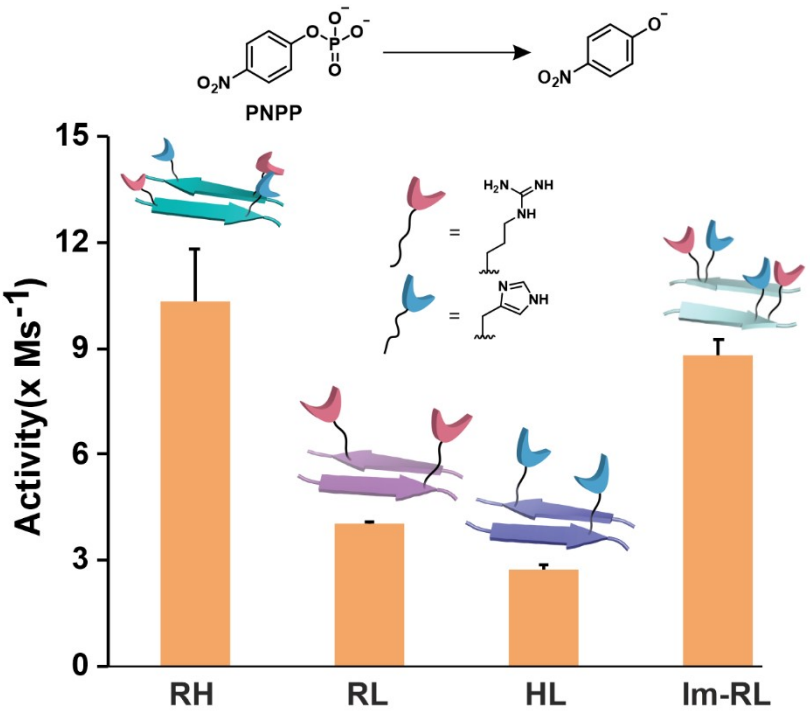

Figure S11. Bar diagram of initial rates of hydrolysis of PNPP in different self-assembled systems, [catalyst]=100 μM, [PNPP]=500 μM.

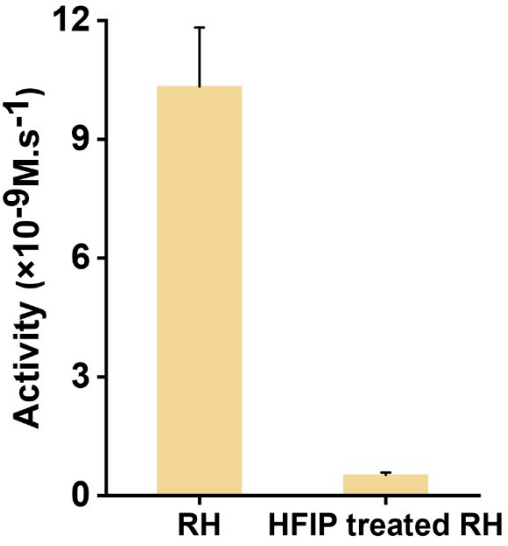

Figure S12. Bar diagram of activity of PNPP hydrolysis by **RH** and HFIP treated **RH**. [Catalyst]=100 μM, [PNPP]=500 μM.

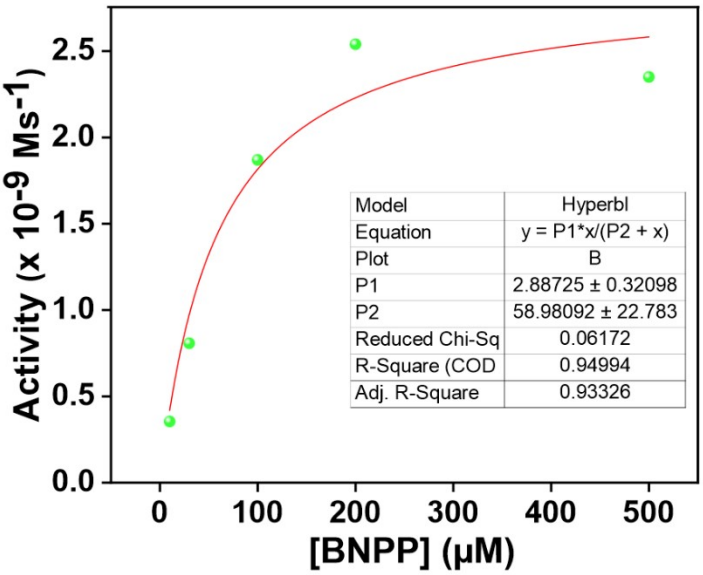

Figure S13. Representative Michaelis-Menten plot of **RH** for BNPP substrate.

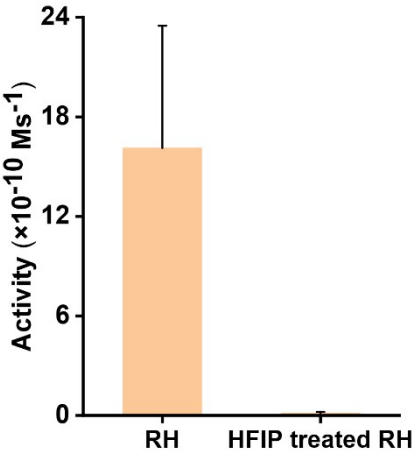

Figure S14. Bar diagram of activity of BNPP hydrolysis by **RH** and HFIP treated **RH**. [Catalyst]=100 μM, [BNPP]=500 μM.

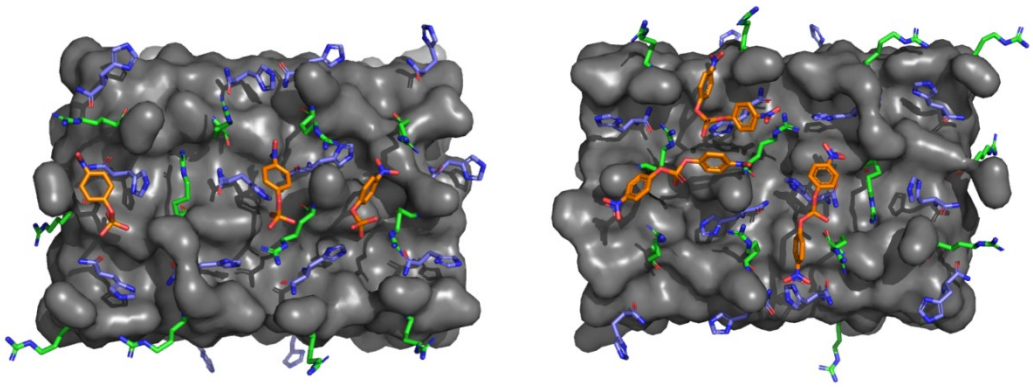

Figure S15. Substrate molecules PNPP and BNPP docked onto the surface of an equilibrated model of RH assembly obtained from MD simulations.

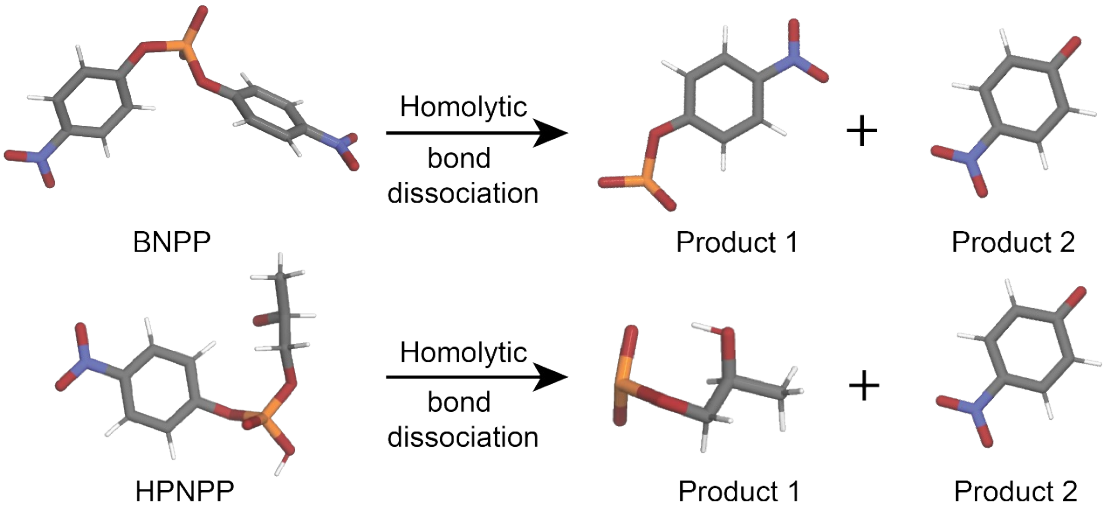

Figure S16. Structures of reactants and products resulting from the homolytic cleavage of phosphoester bond of BNPP and HPNPP.

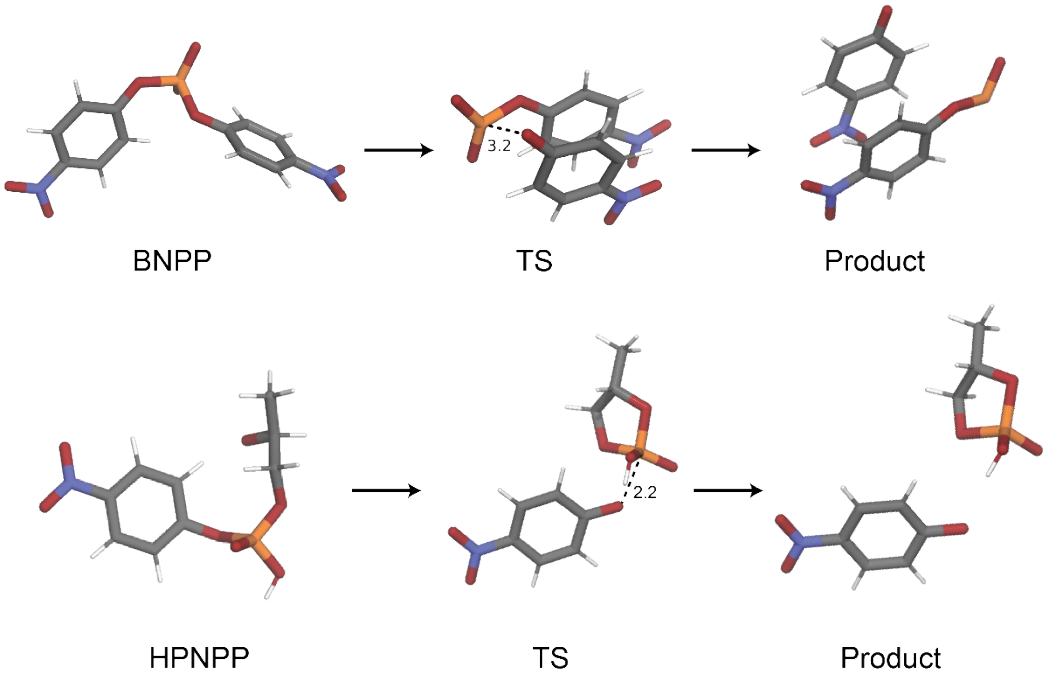

Substrate	Free energy of activation
BNPP	50.0 Kcal.mol $^{-1}$
HPNPP	18.4 Kcal.mol^{-1}

Figure S17. Structures of reactants, transition state and products for uncatalyzed reaction for BNPP and HPNPP and their free energy for activation [distances are in angstrom (Å)].

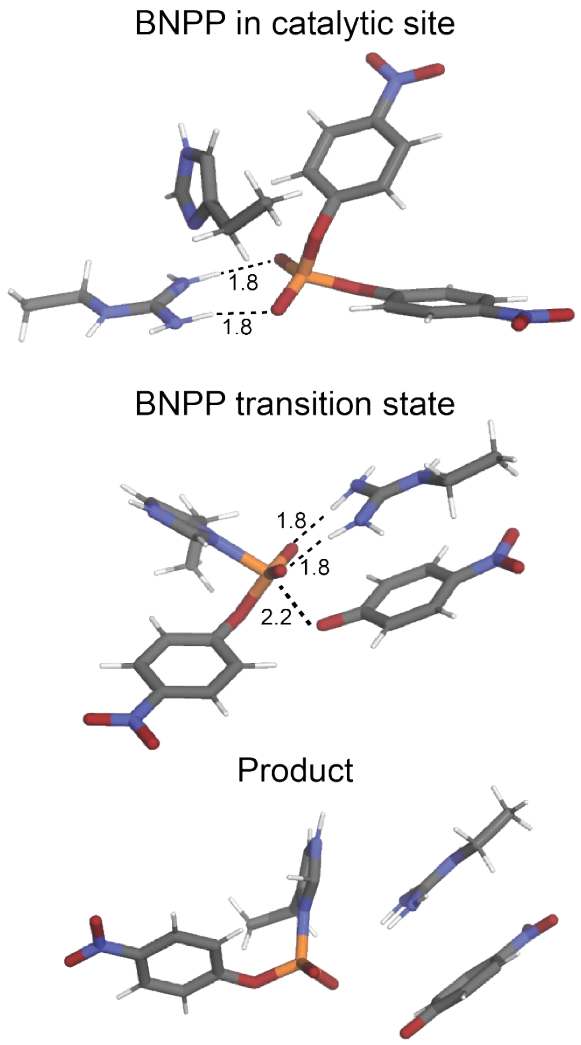

Figure S18. Structures of BNPP reactants and products and transition state for catalysed reaction [distances are in angstrom (Å)].

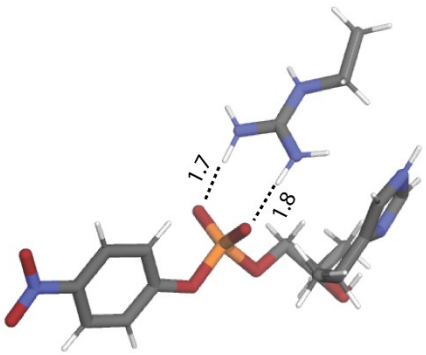

Figure S19. Structures of HPNPP reactant in catalytic reaction site [distances are in angstrom (Å)].

XYZ Coordinaates

Homolytic cleavage

BNPP Reactant

C	-2.09655	-0.05809	-0.58100
C	-3.06237	-1.04388	-0.71772
C	-4.27229	-0.91241	-0.04546
C	-4.54873	0.18488	0.76580
C	-3.58440	1.16714	0.90215
C	-2.35809	1.05236	0.23352
H	-1.15633	-0.13723	-1.11064
H	-5.50110	0.25776	1.27583
H	-3.75749	2.03681	1.52579
H	-2.88403	-1.91073	-1.34191
N	-5.28107	-1.95260	-0.19470
O	-5.02260	-2.90933	-0.90850
O	-6.33864	-1.81879	0.40146
O	-1.48121	2.06592	0.44430
P	0.03491	2.17351	-0.22091
O	-0.01486	1.89121	-1.68209
O	0.61508	0.82376	0.58381
O	0.65129	3.39104	0.36241
C	1.84747	0.30268	0.37205
C	2.34796	-0.52666	1.38532
C	3.59329	-1.11360	1.25263
C	4.33201	-0.85992	0.09940
C	3.85062	-0.04447	-0.91864
C	2.59861	0.53739	-0.78823
H	2.19223	1.15565	-1.57933
N	5.64675	-1.46995	-0.04539
H	4.45091	0.12347	-1.80426
H	1.74291	-0.69301	2.26933
H	3.99741	-1.75496	2.02587
O	6.05166	-2.18625	0.85727
O	6.28264	-1.23691	-1.06181

Product 1 after homolytic cleavage

C	1.41434	1.24461	0.00009
C	0.04381	1.23875	0.00055
C	-0.61705	0.00015	-0.00044
C	0.04386	-1.23846	-0.00223
C	1.41439	-1.24494	-0.00208
C	2.16675	-0.00015	-0.00008
H	1.97859	2.17046	0.00014
H	-0.53530	-2.15304	-0.00352
H	1.97796	-2.17126	-0.00296
H	-0.53505	2.15355	0.00181
N	-2.08324	-0.00000	0.00035
O	-2.65076	1.07866	-0.00251
O	-2.65047	-1.07880	0.00388
O	3.41372	0.00020	0.00203

Product 2 after homolytic cleavage

P	-3.18231	-0.25356	-0.27937
O	-3.03569	-1.48204	0.58322
O	-1.89705	0.82653	0.12912
O	-4.38487	0.64766	-0.22140
C	-0.59389	0.50064	0.08517
C	0.31577	1.57180	0.14774
C	1.67771	1.34286	0.10676
C	2.13321	0.02990	-0.00369
C	1.25394	-1.04652	-0.06521
C	-0.11201	-0.81669	-0.01496
H	-0.81066	-1.64340	-0.03105
N	3.56353	-0.22077	-0.05096
H	1.64366	-2.05410	-0.14416
H	-0.07693	2.57942	0.22566
H	2.38663	2.16022	0.15378
O	4.32102	0.73669	0.01613
O	3.94644	-1.37700	-0.15604

HPNPP Reactant

C	-1.17407	0.34127	0.53990
C	-2.43992	0.90501	0.49868
C	-3.48675	0.19289	-0.07697
C	-3.30367	-1.07808	-0.61551
C	-2.04009	-1.63914	-0.57488
C	-0.97053	-0.93643	-0.00196
H	-0.35182	0.87426	0.99949
H	-4.13964	-1.60709	-1.05579
H	-1.85374	-2.62506	-0.98547
H	-2.62151	1.88980	0.91112
N	-4.81285	0.79242	-0.11553
O	-4.95551	1.90996	0.35675
O	-5.72188	0.14971	-0.61868
O	0.22434	-1.57348	-0.01565
P	1.65639	-0.90637	0.51632
O	1.50884	-0.36814	1.89991
O	1.70323	0.30809	-0.57224
O	2.69913	-1.92565	0.16786
C	2.63813	1.36634	-0.35921
C	4.06715	0.85657	-0.15010
C	5.05587	2.00477	-0.24946
O	4.40212	-0.11192	-1.12287
H	3.88676	-0.91023	-0.88048
H	2.32532	1.97449	0.49868
H	2.59618	1.97976	-1.26431
H	4.12898	0.41263	0.85620
H	4.81371	2.79521	0.46693
H	5.03224	2.42829	-1.25881
H	6.06886	1.64877	-0.04718

Product 1 after homolytic cleavage

P	-1.65854	-0.00818	0.07054
O	-1.73117	-1.02926	-1.04365
O	-0.51181	-0.49675	1.17454

O	-1.36056	1.45595	-0.24098
C	0.74663	-0.95277	0.67581
C	1.39480	0.04417	-0.28766
C	2.83998	-0.33773	-0.55607
O	1.36684	1.35248	0.24738
H	0.42184	1.61847	0.20708
H	0.63023	-1.92494	0.18023
H	1.38814	-1.07970	1.55493
H	0.82904	0.01623	-1.23255
H	2.91128	-1.35439	-0.95376
H	3.41699	-0.28555	0.37316
H	3.28579	0.35123	-1.27786

Product 2 after homolytic cleavage

C	1.41434	1.24461	0.00009
C	0.04381	1.23875	0.00055
C	-0.61705	0.00015	-0.00044
C	0.04386	-1.23846	-0.00223
C	1.41439	-1.24494	-0.00208
C	2.16675	-0.00015	-0.00008
H	1.97859	2.17046	0.00014
H	-0.53530	-2.15304	-0.00352
H	1.97796	-2.17126	-0.00296
H	-0.53505	2.15355	0.00181
N	-2.08324	-0.00000	0.00035
O	-2.65076	1.07866	-0.00251
O	-2.65047	-1.07880	0.00388
O	3.41372	0.00020	0.00203

For uncatalyzed reactions

BNPP reactant

C	-2.09655	-0.05809	-0.58100
C	-3.06237	-1.04388	-0.71772

C	-4.27229	-0.91241	-0.04546
C	-4.54873	0.18488	0.76580
C	-3.58440	1.16714	0.90215
C	-2.35809	1.05236	0.23352
H	-1.15633	-0.13723	-1.11064
H	-5.50110	0.25776	1.27583
H	-3.75749	2.03681	1.52579
H	-2.88403	-1.91073	-1.34191
N	-5.28107	-1.95260	-0.19470
O	-5.02260	-2.90933	-0.90850
O	-6.33864	-1.81879	0.40146
O	-1.48121	2.06592	0.44430
P	0.03491	2.17351	-0.22091
O	-0.01486	1.89121	-1.68209
O	0.61508	0.82376	0.58381
O	0.65129	3.39104	0.36241
C	1.84747	0.30268	0.37205
C	2.34796	-0.52666	1.38532
C	3.59329	-1.11360	1.25263
C	4.33201	-0.85992	0.09940
C	3.85062	-0.04447	-0.91864
C	2.59861	0.53739	-0.78823
H	2.19223	1.15565	-1.57933
N	5.64675	-1.46995	-0.04539
H	4.45091	0.12347	-1.80426
H	1.74291	-0.69301	2.26933
H	3.99741	-1.75496	2.02587
O	6.05166	-2.18625	0.85727
O	6.28264	-1.23691	-1.06181

Transition state

C	1.98929	-1.30838	0.76622
C	0.68069	-1.25100	1.24376
C	-0.39195	-1.67997	0.45732
C	-0.14985	-2.20350	-0.84272

C	1.11612	-2.28910	-1.33242
C	2.30173	-1.89647	-0.55986
H	2.82364	-1.16913	1.45051
H	-1.01270	-2.52020	-1.43230
H	1.30927	-2.70854	-2.32425
H	0.47537	-0.86656	2.24303
N	-1.73346	-1.54239	0.91450
O	-1.93976	-1.12464	2.05385
O	-2.65786	-1.81542	0.13700
O	3.46591	-2.05566	-1.00575
P	2.96097	1.21591	0.38036
O	2.58918	1.64381	1.74731
O	1.83873	1.41626	-0.75078
O	4.27726	1.01135	-0.25460
C	0.46780	1.35104	-0.56700
C	-0.24432	0.92007	-1.68453
C	-1.61503	0.79537	-1.60434
C	-2.24512	1.11774	-0.40698
C	-1.54329	1.55436	0.70598
C	-0.15941	1.69337	0.62609
H	0.42401	2.00899	1.47885
N	-3.69582	0.97088	-0.30518
H	-2.07434	1.76220	1.62413
H	0.30772	0.63851	-2.57742
H	-2.20915	0.43537	-2.43552
O	-4.29825	0.62620	-1.30704
O	-4.22018	1.23873	0.76343

Product

C	1.69427	1.61422	-0.50135
C	0.71056	1.01374	-1.24945
C	-0.61786	1.39407	-1.02591
C	-1.00892	2.37198	-0.09221
C	-0.03612	2.99032	0.64464
C	1.36623	2.63599	0.47768

H	2.73432	1.32207	-0.60458
H	-2.05923	2.60350	0.03210
H	-0.27613	3.75226	1.37875
H	0.95454	0.21926	-1.94452
N	-1.66778	0.70466	-1.77797
O	-1.32961	-0.03640	-2.68432
O	-2.82661	0.89791	-1.44351
O	2.25401	3.18636	1.16103
P	3.27387	-1.56863	-0.19698
O	2.59816	-1.32070	-1.52301
O	2.15342	-1.15775	1.04992
O	4.51137	-0.82849	0.23333
C	0.81451	-1.20070	0.94961
C	0.10223	-0.43205	1.88643
C	-1.27763	-0.36094	1.83462
C	-1.94798	-1.07740	0.84522
C	-1.26687	-1.88182	-0.06516
C	0.11644	-1.94902	-0.01378
H	0.66136	-2.53348	-0.74272
N	-3.39371	-0.96274	0.74457
H	-1.82187	-2.42894	-0.81790
H	0.66182	0.12837	2.62761
H	-1.83535	0.25409	2.53014
O	-3.96557	-0.19612	1.50502
O	-3.96891	-1.63126	-0.09999

HPNPP Reactant

C	-1.24636	-1.04597	0.07266
C	-2.53522	-0.68446	0.47734
C	-3.06066	0.58248	0.16111
C	-2.26228	1.47584	-0.57669
C	-0.97564	1.11132	-0.98116
C	-0.44948	-0.14429	-0.65727
H	-0.90394	-2.03433	0.32598
H	-2.63214	2.45783	-0.84288
H	-0.37904	1.81502	-1.54858

H	-3.12364	-1.40113	1.03626
N	-4.37812	0.95131	0.57531
O	-5.05270	0.18861	1.19966
O	-4.82005	2.02689	0.30258
O	0.80572	-0.42813	-1.08834
P	1.89902	-1.64457	-0.52926
O	1.36936	-2.34135	0.75279
O	3.44447	-0.93105	-0.11827
O	2.13182	-2.86413	-1.74199
C	3.25720	0.16075	0.75951
C	3.67958	1.46036	0.06672
C	3.56551	2.65151	1.01614
O	2.87470	1.68483	-1.05240
H	3.89881	-0.00874	1.65051
H	2.21655	0.26758	1.14713
H	4.73653	1.36804	-0.26502
H	4.21756	2.50105	1.90290
H	2.51519	2.77901	1.35600
H	3.88670	3.57901	0.49629
H	1.23269	-3.25627	-1.87889

Transition state

C	-1.01876	0.19517	0.61620
C	-2.24941	0.81244	0.60036
C	-3.34704	0.16345	0.02154
C	-3.21064	-1.11212	-0.53998
C	-1.98031	-1.72884	-0.52393
C	-0.83251	-1.10540	0.05280
H	-0.16756	0.69757	1.06220
H	-4.07432	-1.59506	-0.98235
H	-1.85136	-2.71659	-0.95454
H	-2.38412	1.79730	1.03249
N	-4.62498	0.81153	0.00457
O	-4.72616	1.93327	0.49645
O	-5.57916	0.22494	-0.50171

O	0.29776	-1.73525	0.06548
P	2.29674	-0.85732	0.10584
O	1.90450	-0.75772	1.67453
O	1.51667	0.22660	-0.83202
O	2.79823	-2.13711	-0.45319
C	2.27402	1.41849	-1.06126
C	3.29706	1.47996	0.06963
C	4.53641	2.28085	-0.26171
O	3.63619	0.11229	0.26981
H	1.58467	2.26490	-1.06555
H	2.77423	1.34166	-2.03358
H	2.81588	1.86842	0.97911
H	4.27155	3.32238	-0.46597
H	5.02654	1.86112	-1.14492
H	5.23960	2.26041	0.57413
H	1.09154	-1.28316	1.78268

Product

C	-1.38223	-0.25949	0.67957
C	-2.51207	0.56403	0.67417
C	-3.67287	0.18449	-0.03034
C	-3.66897	-1.04073	-0.72791
C	-2.53609	-1.86018	-0.71968
C	-1.39311	-1.47092	-0.01692
H	-0.49940	0.04633	1.22623
H	-4.54162	-1.36582	-1.27994
H	-2.54800	-2.79841	-1.26013
H	-2.47749	1.49739	1.22149
N	-4.82963	1.02407	-0.03698
O	-4.82871	2.06133	0.55517
O	-5.81121	0.69828	-0.63437
O	-0.30627	-2.26149	-0.01117
P	2.98957	-0.64876	0.47976
O	2.47862	-1.06949	2.08436
O	1.79044	0.23042	-0.39940

O	3.40097	-1.89969	-0.34140
C	2.55877	1.27919	-0.92173
C	3.66632	1.64088	0.09097
C	4.67206	2.61686	-0.51378
O	4.31129	0.46226	0.49207
H	1.91982	2.16576	-1.12026
H	3.00518	0.93897	-1.88394
H	3.20506	2.11375	0.98900
H	4.16062	3.55540	-0.81620
H	5.16257	2.16744	-1.40361
H	5.45262	2.86418	0.23652
H	1.54901	-1.39189	1.97553

Catalysed Reactions

BNPP Reactant

C	-8.19173	-1.57997	-0.73213
C	-6.78782	-1.27040	-1.22654
N	-5.81005	-1.98811	-0.41461
C	-4.48521	-1.82425	-0.52007
N	-3.98695	-0.99456	-1.43020
N	-3.66707	-2.53214	0.26514
H	-8.40870	-2.64849	-0.82186
H	-8.92221	-1.03290	-1.33081
H	-6.68716	-1.55685	-2.28086
H	-6.58613	-0.19681	-1.14337
H	-6.14091	-2.76250	0.14735
H	-4.58509	-0.59533	-2.13797
H	-2.99091	-0.72845	-1.42507
H	-4.04461	-2.90483	1.12636
H	-2.66418	-2.30314	0.26949
C	-0.12135	0.46579	3.63689
C	-1.34238	-0.13449	2.94450
C	-2.08242	0.85893	2.09975
C	-2.14182	2.22596	2.22106

N	-2.86246	0.45310	1.03788
C	-3.38687	1.55154	0.53746
N	-2.98296	2.65046	1.21991
H	-0.40673	1.28011	4.31133
H	-1.04396	-0.96144	2.29316
H	-2.02234	-0.55397	3.69835
H	-1.67554	2.91919	2.90380
H	-4.05436	1.60740	-0.31185
H	-3.23795	3.60731	1.01808
P	-0.37394	-1.03299	-0.70103
C	4.54902	-1.99251	-1.37397
N	5.97470	-2.85119	0.43102
O	0.98335	-1.41869	-1.57956
C	4.65761	-2.48765	-0.07787
N	2.28134	5.05091	-0.82501
O	0.31506	-0.01274	0.38781
C	3.54913	-2.64919	0.74667
O	-1.25428	-0.32592	-1.67580
C	2.29331	-2.30481	0.26897
O	-0.83921	-2.21192	0.08950
C	2.16974	-1.79199	-1.02880
O	6.05543	-3.26601	1.57627
C	3.29635	-1.64301	-1.84716
O	6.93429	-2.72295	-0.31359
C	0.78245	1.22284	0.03650
O	3.46723	5.26226	-0.62899
C	-0.08583	2.20121	-0.45272
O	1.50483	5.88734	-1.25742
C	0.40906	3.46391	-0.73894
C	1.76075	3.71899	-0.52485
C	2.63419	2.75600	-0.03162
C	2.13527	1.49253	0.25171
H	5.43357	-1.88096	-1.98898
H	3.67395	-3.04439	1.74705
H	1.41407	-2.43319	0.88928
H	3.16641	-1.24416	-2.84670

H	-1.12989	1.95065	-0.59976
H	-0.23600	4.24782	-1.11591
H	3.67815	2.99749	0.12285
H	2.77708	0.70863	0.64060
H	0.57920	0.86838	2.89812
H	0.40209	-0.28829	4.23133
H	-8.30686	-1.28332	0.31361

Transition state

C	6.59236	0.05227	2.22079
C	5.07855	-0.07645	2.17997
N	4.50805	0.95213	1.31161
C	3.20024	1.05838	1.05869
N	2.36050	0.14839	1.54987
N	2.71691	2.11009	0.38490
H	7.01679	-0.10738	1.22578
H	7.00188	-0.70187	2.89556
H	4.81095	-1.06949	1.79628
H	4.64851	0.02763	3.18211
H	5.14041	1.59625	0.85386
H	2.73157	-0.74473	1.84311
H	1.36392	0.15060	1.28566
H	3.37508	2.76732	-0.01094
H	1.82515	2.00708	-0.11795
C	-2.70502	3.39378	-2.33304
C	-1.93793	3.95506	-1.13093
C	-2.26859	3.26777	0.15753
C	-3.08778	3.70449	1.16025
N	-1.77335	2.03072	0.55012
C	-2.27742	1.74085	1.74334
N	-3.07726	2.73393	2.13546
H	-3.78492	3.46356	-2.16810
H	-0.86307	3.87513	-1.30601
H	-2.18052	5.01449	-1.00358
H	-3.65483	4.61576	1.26319

H	-2.06104	0.84389	2.30084
H	-3.57744	2.76517	3.01497
P	-0.66550	0.77993	-0.37941
C	3.31842	-2.38699	-0.51380
N	5.60283	-1.50706	-0.66260
O	0.18883	-0.89411	-1.56304
C	4.21374	-1.41197	-0.98044
N	-5.94202	-2.97927	0.71520
O	-1.96224	0.35294	-1.29289
C	3.75711	-0.30912	-1.71747
O	-0.36560	-0.04208	0.83824
C	2.41082	-0.15324	-1.94336
O	0.23125	1.76153	-1.06153
C	1.45215	-1.08344	-1.42806
O	6.36263	-0.62316	-1.06002
C	1.96961	-2.22965	-0.74285
O	5.99788	-2.45145	0.02138
C	-2.91937	-0.47552	-0.77048
O	-7.05936	-2.50986	0.85726
C	-2.61358	-1.80487	-0.47213
O	-5.65117	-4.13400	0.98090
C	-3.61263	-2.63193	0.01781
C	-4.88949	-2.10649	0.19712
C	-5.20428	-0.78385	-0.09454
C	-4.20122	0.04246	-0.58175
H	3.70018	-3.23922	0.03778
H	4.47425	0.42088	-2.07603
H	2.03545	0.70954	-2.48090
H	1.25834	-2.96120	-0.37134
H	-1.59842	-2.14739	-0.64096
H	-3.41721	-3.66955	0.25795
H	-6.21049	-0.41711	0.06427
H	-4.39323	1.08466	-0.81772
H	-2.44983	2.34579	-2.50359
H	-2.46023	3.96205	-3.23459
H	6.88973	1.03893	2.58703

Product

C	5.79349	1.25011	3.23163
C	4.63329	0.53486	2.54605
N	3.98800	1.39758	1.57595
C	2.88082	0.96454	0.78352
N	2.35228	-0.35045	0.92031
N	2.35871	1.77210	-0.07482
H	6.55305	1.55344	2.47981
H	6.27039	0.56857	3.96714
H	5.02725	-0.36949	2.03412
H	3.89536	0.22756	3.31821
H	4.34339	2.35739	1.44203
H	2.74382	-1.02388	1.59205
H	1.56612	-0.66133	0.33241
H	2.72522	2.72750	-0.19577
H	1.56556	1.47793	-0.66208
C	-2.74597	2.97506	-1.22457
C	-1.29104	2.93734	-0.77343
C	-1.07648	2.05798	0.43588
C	-0.74648	2.52245	1.63260
N	-1.13339	0.63889	0.49287
C	-0.80798	0.21307	1.83154
N	-0.58675	1.45181	2.52987
H	-3.39419	3.33547	-0.39748
H	-0.62742	2.60656	-1.59957
H	-1.01484	3.98352	-0.51527
H	-0.61220	3.56372	1.89579
H	-1.65670	-0.33899	2.28426
H	-0.33182	1.54076	3.52357
P	-1.38309	-0.50885	-0.86010
C	4.91137	-1.74944	-0.84423
N	6.29077	0.29557	-0.89352
O	1.82522	-2.60754	-2.59221
C	5.15241	-0.44898	-1.33220

N	-7.94988	-1.29516	0.77856
O	-2.93995	-0.37015	-1.57995
C	4.24429	0.10371	-2.25836
O	-1.08923	-2.13667	-0.33290
C	3.12716	-0.62372	-2.68007
O	-0.32521	-0.17772	-1.94557
C	2.90077	-1.91099	-2.18672
O	6.48572	1.40078	-1.30202
C	3.79318	-2.47293	-1.27022
O	7.05697	-0.17577	-0.10788
C	-4.12889	-0.60820	-0.97194
O	-8.94705	-1.09328	0.15290
C	-4.23358	-1.07661	0.35051
O	-8.04028	-1.69182	1.90152
C	-5.48805	-1.30181	0.92457
C	-6.66685	-1.06520	0.19192
C	-6.55432	-0.59797	-1.13128
C	-5.29868	-0.37411	-1.70225
H	5.58559	-2.20632	-0.13122
H	4.39529	1.09993	-2.65388
H	2.43704	-0.18478	-3.38957
H	3.62011	-3.46995	-0.88521
H	-3.35697	-1.27428	0.94679
H	-5.53492	-1.66260	1.94425
H	-7.43764	-0.40481	-1.72656
H	-5.23483	-0.01369	-2.72148
H	-3.09740	1.98681	-1.55101
H	-2.84709	3.67126	-2.08363
H	5.42555	2.15226	3.76511

HPNPP

Reactant

C	5.43669	4.15571	-0.51049
C	4.42977	3.09314	-0.10291

N	3.32278	3.06712	-1.05350
C	2.22660	2.31443	-0.89922
N	2.10315	1.53016	0.16929
N	1.24422	2.37115	-1.80004
H	5.86206	3.93207	-1.49299
H	6.25197	4.18713	0.21515
H	4.91186	2.10865	-0.06818
H	4.03115	3.31493	0.89295
H	3.44993	3.54194	-1.93806
H	2.86643	1.42176	0.82508
H	1.22360	1.02012	0.35767
H	1.34156	2.97746	-2.60191
H	0.47936	1.67760	-1.82011
C	0.60278	-1.18931	3.33966
C	1.49013	-1.86103	2.29610
C	2.77628	-1.12588	2.07219
C	3.30742	-0.06489	2.76068
N	3.64128	-1.49101	1.05848
C	4.66623	-0.66997	1.13053
N	4.50669	0.21965	2.13979
H	0.33088	-0.18176	3.00931
H	1.72214	-2.89169	2.59757
H	0.96056	-1.92521	1.33986
H	2.95562	0.50368	3.60731
H	5.53560	-0.67369	0.48797
H	5.18280	0.91145	2.43690
N	-7.05269	1.08505	0.52574
P	-0.71151	-0.48185	-0.81820
C	-4.60494	1.23136	0.44900
O	-2.14732	-1.27849	-0.62450
C	-5.75733	0.48641	0.22822
O	0.12116	-1.82329	-1.16087
C	-5.71331	-0.81588	-0.26263
O	2.33375	-3.51640	-0.48174
C	-4.48097	-1.37604	-0.54653
O	-0.78064	0.42773	-2.01264

C	-3.30973	-0.64021	-0.33101
O	-0.27760	0.11387	0.49334
C	-3.36918	0.66417	0.17625
O	-8.04900	0.39091	0.39728
C	1.44674	-1.58994	-1.65544
O	-7.07947	2.25066	0.88941
C	2.18371	-2.91668	-1.75157
C	3.53340	-2.71418	-2.43564
H	-4.67980	2.23846	0.83980
H	-6.63068	-1.36825	-0.42204
H	-4.40078	-2.38325	-0.93898
H	-2.45811	1.21736	0.37160
H	1.38565	-1.10733	-2.63801
H	1.99134	-0.92942	-0.96542
H	1.56766	-3.60371	-2.34512
H	4.07095	-3.66456	-2.47489
H	3.41743	-2.33480	-3.45506
H	4.14006	-1.99963	-1.86672
H	2.89804	-2.90821	0.04710
H	4.96434	5.14092	-0.54538
H	1.11030	-1.11815	4.30778
H	-0.32027	-1.75817	3.48598

Reference:

1) N. Kapil, A. Singh, M. Singh and D. Das, *Angew. Chem., Int. Ed.,* 2016, **55**, 7772-7776.
2) D. M. Brown and D. A. Usher, *J. Chem. Soc.,* 1965, 6558-6564.
3) C. M. Rufo, Y. S. Moroz, O. V. Moroz, J. Stöhr, T. A. Smith, X. Hu, W. F. DeGrado and I. V. Korendovych, *Nat. Chem.,* 2014, **6**, 303-309.
4) J. Huang and A. D. MacKerell Jr, *J. Comput. Chem.,* 2013, **34**, 2135-2145.
5) W. L. Jorgensen, J. Chandrasekhar, J. D. Madura, R. W. Impey and M. L. Klein, *J. Chem. Phys.,* 1983, **79**, 926-935.
6) M. J. Abraham, T. Murtola, R. Schulz, S. Páll, J. C. Smith, B. Hess and E. Lindahl, *SoftwareX,* 2015, **1**, 19-25.
7) U. Essmann, L. Perera, M. L. Berkowitz, T. Darden, H. Lee, L. G. Pedersen, *J. Chem. Phys.,* 1995, **103**, 8577-8593.

8) B. Hess, H. Bekker, H. J. C. Berendsen and J. G. E. M. Fraaije, *J. Comput. Chem.,* 1997, **18**, 1463-1472.
9) G. Bussi, D. Donadio and M. Parrinello, *J. Chem. Phys.,* 2007, **126**, 14101.
10) M. Parrinello and A. Rahman, *J. Appl. Phys.,* 1981, **52**, 7182-7190.
11) O. Trott and A. J. Olson, *J. Comput. Chem.,* 2010, **31**, 455-461.
12) M. F. Adasme, K. L. Linnemann, S. N. Bolz, F. Kaiser, S. Salentin, V. J. Haupt and M. Schroeder, *Nucleic Acids Res.,* 2021, **49**, 530-534.
13) M. J. Frisch, G. W. Trucks, H. B. Schlegel, G. E. Scuseria, M. A. Robb, J. R. Cheeseman, G. Scalmani, V. Barone, G. A. Petersson, H. Nakatsuji, X. Li, M. Caricato, A. V. Marenich, J. Bloino, B. G. Janesko, R. Gomperts, B. Mennucci, H. P. Hratchian, J. V. Ortiz, A. F. Izmaylov, J. L. Sonnenberg, D. Williams-Young, F. Ding, F. Lipparini, F. Egidi, J. Goings, B. Peng, A. Petrone, T. Henderson, D. Ranasinghe, V. G. Zakrzewski, J. Gao, N. Rega, G. Zheng, W. Liang, M. Hada, M. Ehara, K. Toyota, R. Fukuda, J. Hasegawa, M. Ishida, T. Nakajima, Y. Honda, O. Kitao, H. Nakai, T. Vreven, K. Throssell, J. A. Montgomery, Jr., J. E. Peralta, F. Ogliaro, M. J. Bearpark, J. J. Heyd, E. N. Brothers, K. N. Kudin, V. N. Staroverov, T. A. Keith, R. Kobayashi, J. Normand, K. Raghavachari, A. P. Rendell, J. C. Burant, S. S. Iyengar, J. Tomasi, M. Cossi, J. M. Millam, M. Klene, C. Adamo, R. Cammi, J. W. Ochterski, R. L. Martin, K. Morokuma, O. Farkas, J. B. Foresman and D. J. Fox, *Gaussian 16*, 2016.
14) L. Gabrielli, L. J. Prins, F. Rastrelli, F. Mancin and P. Scrimin, *Eur. J. Org. Chem.,* 2020, **32**, 5044-5055.
15) L. F. Olguin, S. E. Askew, A. C. O'Donoghue and F. Hollfelder, *J. Am. Chem. Soc.,* 2008, **130***,* 16547-16555.
16) T. Koike and E. Kimura, *J. Am. Chem. Soc.,* 1991, **113***,* 8935-8941.